Voltage-Jump Relaxation Kinetics for Wild-type and Chimeric β Subunits of Neuronal Nicotinic Receptors

ANTONIO FIGL,* CESAR LABARCA,‡ NORMAN DAVIDSON,‡ HENRY A. LESTER,‡ and BRUCE N. COHEN§

From the *Division of Chemistry and Chemical Engineering; ‡Division of Biology, California Institute of Technology, Pasadena, California 91125; and §Division of Biomedical Sciences, University of California at Riverside, Riverside, California 92521-0121

ABSTRACT We have studied the voltage-jump relaxation currents for a series of neuronal nicotinic acetylcholine receptors resulting from the coexpression of wild-type and chimeric β4/β2 subunits with α3 subunits in *Xenopus* oocytes. With acetylcholine as the agonist, the wild-type α3β4 receptors displayed five- to eightfold slower voltage-jump relaxations than did the wild-type α3β2 receptors. In both cases, the relaxations could best be described by two exponential components of approximately equal amplitudes over a wide range of [ACh]'s. Relaxation rate constants increased with [ACh] and saturated at 20- to 30-fold lower concentrations for the α3β2 receptor than for the α3β4 receptor, as observed previously for the peak steady state conductance. Furthermore, the chimeric β4/β2 subunits showed a transition in the concentration dependence of the rate constants in the region between residues 94 and 109, analogous to our previous observation with steady state conductances. However, our experiments with a series of β-subunit chimeras did not localize residues that govern the absolute value of the kinetic parameters. Hill coefficients for the relaxations also differed from those previously measured for steady state responses. The data reinforce previous conclusions that the region between residues 94 and 109 on the β subunit plays a role in binding agonist but also show that other regions of the receptor control gating kinetics subsequent to the binding step.

INTRODUCTION

Both the α and β subunits contribute to the pharmacological and biophysical properties of neuronal nicotinic acetylcholine receptors (neuronal nAChRs) (Papke et al., 1989; Luetje et al., 1990; Luetje and Patrick, 1991; Papke and Heinemann, 1991; Charnet et al., 1991; Figl et al., 1992; Papke et al., 1993; Wong et al., 1993; Cohen et al., 1995; reviewed in Role, 1992; Papke, 1993; Sargent, 1993). At the single-channel level, parameters such as open time, burst duration, and conductance depend on the particular combination of α and β subtypes that form the receptor (Papke et al., 1989, 1991; reviewed in Papke, 1993). Specifically, the α2, α3, and α4 subunits produce channels with different open times, burst durations, and conductances when coexpressed with the β2 subunit in *Xenopus* oocytes (Papke et al., 1989). The β subunit appears to play a major role in determining the bursting behavior of single channels (Papke et al., 1991). However, we have no information about its effects on the macroscopic kinetics of neuronal nAChRs. To test the role of the β subunit in the macroscopic kinetic behavior of neuronal nAChRs, we studied voltage-jump relaxations of the rat α3β2 and α3β4 receptors. Voltage-jump relaxations provide a simple and convenient method of studying the macroscopic kinetics of receptors and may eventually prove useful in identifying the nAChR subtypes in their native tissue. Only the voltage-jump relaxations of the α4β2 receptor have been studied previously (Charnet et al., 1991).

Our previous work showed that residues within the first 109 amino acids of the β4 subunit appear to play a role in determining the sensitivity of neuronal nAChRs to nicotinic agonists (Figl et al., 1992; Cohen et al., 1995). Extending a chimeric β subunit from 94 to 109 β4 NH_2-terminal residues and coexpressing it with the α3 subunit in *Xenopus* oocytes is sufficient to restore (*a*) the relative sensitivities to acetylcholine (ACh), cytisine, and tetramethylammonium (TMA) (Figl et al., 1992; Figl et al., 1993) and (*b*) the half-maximal concentration for channel activation (EC_{50}) by ACh from α3β2-

Address correspondence to Bruce N. Cohen, Division of Biomedical Sciences, University of California at Riverside, Riverside, CA 92521-0121. Fax, (909) 787-5504; E-mail, BRUCE.COHEN@UCR.EDU

J. GEN. PHYSIOL. © The Rockefeller University Press • 0022-1295/96/03/369/11 $2.00
Volume 107 March 1996 369–379

like to α3β4-like levels (Cohen et al., 1995). If this region is involved in agonist binding to the receptor, we would then also expect it to affect the dependence of the relaxation rate constants on the agonist concentration. To test this hypothesis, we measured the relaxation rate constants for a series of α3β4/β2 chimeric receptors over a wide range of ACh concentrations. Our results show that (*a*) the relaxation currents of the α3β2 and α3β4 receptors contain two exponential components, (*b*) the β subunit has a marked effect on the relaxation kinetics of both components across a wide range of ACh concentrations, and (*c*) the concentration dependence of the relaxation rate constants once again implicates the region between residues 94 and 109 in β4 as crucial in the response of the receptor to agonist.

MATERIALS AND METHODS

Construction of Chimeric β Subunits

We used a previously published method to construct our chimeras (Cohen et al., 1995). In brief, the procedure incorporates a two-step PCR protocol (Higuchi, 1990). In the first step, we generated two partially overlapping DNA fragments. In the second step, the two pieces were combined to generate a cassette incorporating the entire NH_2-terminal portion of β4 followed by the shortest possible segment of β2 necessary to reach a convenient restriction site. This cassette was cut by the appropriate restriction enzymes and ligated to an equivalently restricted native β2 cDNA to produce the complete chimeric cDNA. We checked the transition regions of the chimeras by fluorescent dideoxy-terminator sequencing (Applied Biosystems, Inc., Foster City, CA). Finally, we synthesized mRNA in vitro using the Ambion MEGAscript kit (Ambion Corp., Austin, TX) or a previously published method (Guastella et al., 1990).

Oocyte Expression

We prepared *Xenopus* stage V-VI oocytes as described previously (Quick and Lester, 1994). The α and β subunit cRNAs were injected in a stoichiometric ratio of 2:3. After injection we incubated the oocytes for 2–7 d at 18°C in a modified Barth's solution supplemented with 5% horse serum, 50 μg/ml gentamicin and 2.5 mM Na-pyruvate.

ELECTROPHYSIOLOGICAL RECORDINGS

Agonists were applied using a U-tube microperfusion system (Cohen et al., 1995). After applying the agonist, we allowed the response to reach a steady state before initiating the voltage-jump protocol. Fig. 2, *A* and *B*, of Cohen et al. (1995) show examples of α3β2 and α3β4 responses to a variety of [ACh]'s between 1 and 1,000 μM. The holding potential between voltage-clamp episodes was −50 mV. The recording solution consisted of 98 mM NaCl, 1 mM $MgCl_2$ and 5 mM HEPES (pH 7.4); we omitted Ca^{2+} to prevent distortion from the Ca^{2+}-activated Cl^- channels (Vernino et al., 1992). Oocytes expressing endogenous muscarinic currents were not used in our experiments.

Data Collection and Analysis

The responses were filtered at one third to one quarter of the sampling frequency (sampling frequency = 250-3,000 Hz) and analyzed using pCLAMP V. 6.0 software (Axon Instruments, Inc., Foster City, CA). All our relaxations were fit with two exponential components,

$$I(t) = A_1 e^{-t/\tau_1} + A_2 e^{-t/\tau_2} - I_{ss},$$

where t is the time after the start of the voltage jump (in milliseconds); A_1 and A_2 are the amplitudes (in nanoamperes) of the exponential components; τ_1 and τ_2 are the time constants (in milliseconds); and I_{ss} is the extrapolated steady state current as t approaches $+\infty$. I_{relax} is the sum of the relaxation amplitudes A_1 and A_2. We define the instantaneous current I_{inst} as $I_{ss} - I_{relax}$. Relaxation values are expressed as time constants (in milliseconds) or as the reciprocal of this value, rate constants (in s^{-1}). The values of $1/\tau > 100$ μM ACh for the α3β2 fast component, $>1{,}000$ μM ACh for the α3β4 fast component, >50 μM ACh for the α3β2 slow component, and >200 μM ACh for the α3β4 slow component, were not included in our dose–response analysis because they progressively decreased in value. We are unsure about the cause of this phenomenon, but we suspect that agonist self-block may be responsible. To determine the EC_{50}'s and n_{app}'s for the dose–response relations, we fit the data, by weighted nonlinear least-squares regression, to the modified Hill equation:

$$1/\tau = \frac{1/\tau_{max}}{1 + (EC_{50}/[ACh])^{n_{app}}} + 1/\tau_0, \quad (1)$$

where $1/\tau$ was the measured rate constant at agonist concentration [ACh], $1/\tau_0$ was the rate constant at the low-concentration limit and was determined by extrapolation of the dose–response relationships to [ACh] = 0. We fixed n_{app} at the value that best approximated the shape of the curve. Only $1/\tau_{max}$ and EC_{50} were left to vary. To create the normalized curves shown in Fig. 6, we subtracted $1/\tau_0$ from $1/\tau$ and divided the result by $1/\tau_{max}$.

Concentration Dependence of the Relaxations

To analyze the concentration dependence of the kinetics, we used a simple model similar to those employed for extensive voltage-jump studies of muscle nAChRs (Adams, 1975; Neher and Sakmann, 1975; Sheridan and Lester, 1975). The model involves a fast binding step followed by a slower conformational transition that leads to channel opening:

$$R \underset{k_{-1}}{\overset{k_1[A]^n}{\Leftrightarrow}} A_n R \underset{\alpha}{\overset{\beta}{\Leftrightarrow}} A_n R^*,$$

fast *slow*

SCHEME I

where k_1 and k_{-1} represent the forward and backward rate constants of binding, respectively; β and α are the forward and backward rate constants for the channel-opening transition; n is the Hill coefficient; A is the ligand and R the receptor. This scheme, consisting of two transitions, predicts two relaxation rate constants. With our assumption that the β/α transition is slower and rate limiting, the slower relaxation rate constant becomes:

$$1/\tau = \alpha + \frac{\beta}{1 + (K_d/[A])^n} \quad (2)$$

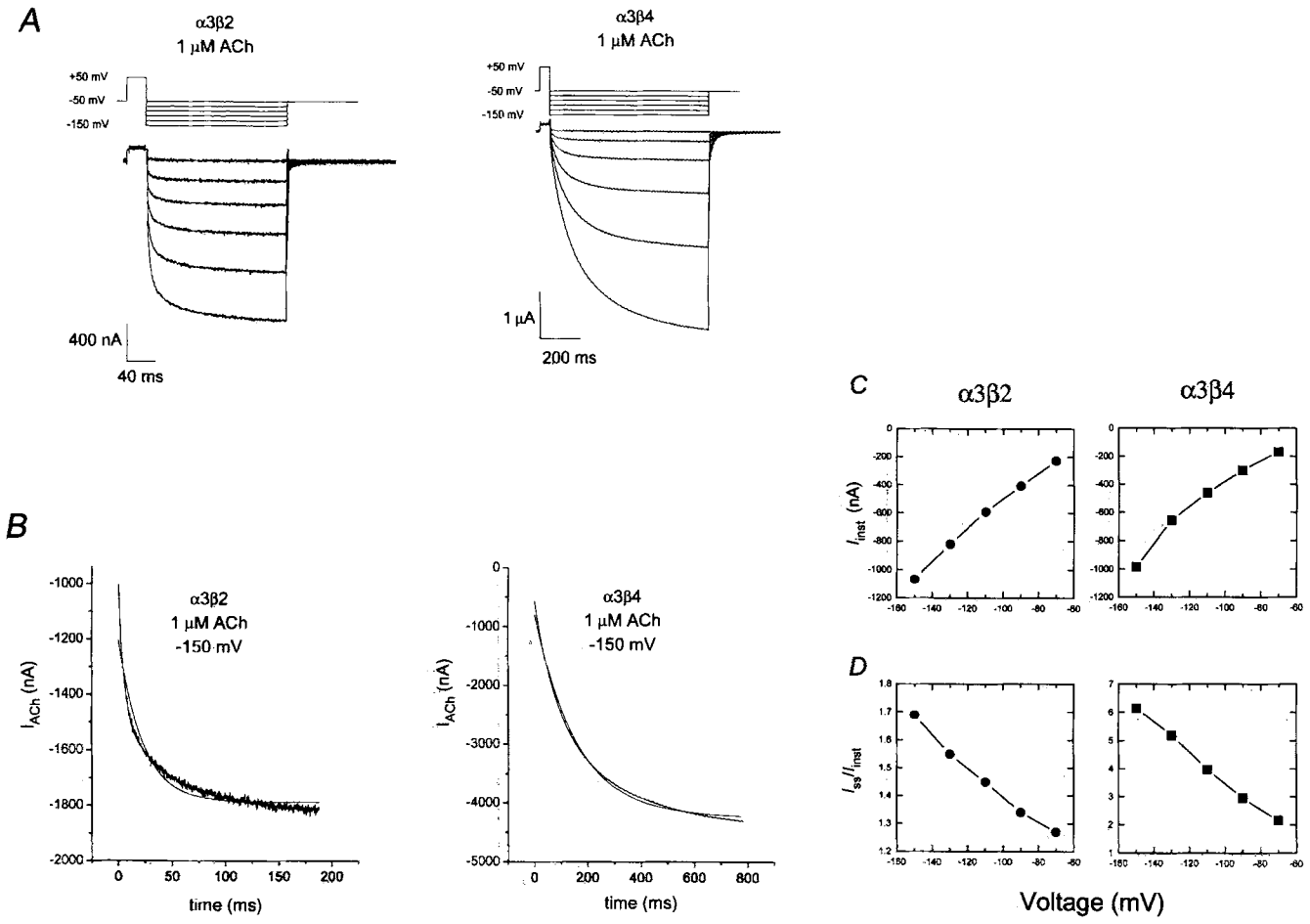

FIGURE 1. Voltage-jump relaxations for the α3β2 (*left column*) and α3β4 (*right column*) receptors expressed in oocytes at [ACh] = 1 μM. (*A*) Voltage-clamp currents. The membrane potential was held at −50 mV, jumped to a prepulse value of +50 mV for 30 or 80 ms (α3β2 or α3β4, respectively), then jumped to various test potentials in the range between −150 and −50 mV in 20-mV increments for 200 or 800 ms (α3β2 or α3β4, respectively). The α3β2 data were filtered at 1 kHz; the α3β4 data were filtered at 250 Hz. ACh-induced currents were isolated by subtracting episodes in the absence of ACh. (*B*) Single and double exponential fits to the α3β2 and α3β4 relaxations at −150 mV. The fit to a single exponential clearly deviates from the data; the fit to two exponentials superimposes on the data. For α3β2, τ_f = 16 ms; τ_s = 75 ms. For α3β4, τ_f = 108 ms; τ_s = 340 ms. (*C*) Instantaneous current-voltage relations for the traces in *A*, obtained by extrapolating the double-exponential fits to the time of the jump to yield I_{inst}. (*D*) Voltage dependence of the steady state values, expressed as I_{ss}/I_{inst}.

where $K_d = k_{-1}/k_1$. According to this assumption, the zero-[ACh] limit is α; the high-[ACh] limit is α + β; and our estimated EC_{50} values equal the dissociation constants (K_d) of Scheme I. Alternatively, we could assume that the binding step in Scheme I is rate limiting. If binding is rate limiting, then one expects the relaxation rate constant to increase proportionally with $[A]^n$. However, if the conformational change is rate limiting, one expects the rate constant to increase hyperbolically or sigmoidally with [*A*] towards a limiting value. Rate-limiting conformational change fits our data better than rate-limiting binding.

RESULTS

The Voltage-Jump Relaxation Procedure

This article describes in detail the voltage dependence of α3β2 and α3β4 receptors. We first describe the framework of our analyses.

Fig. 1 shows sample traces illustrating the voltage-clamp protocol used for most experiments in this study. The ACh concentration was 1 μM. The membrane potential was held at −50 mV, stepped to a prepulse value of +50 mV, then jumped again to various test potentials between −150 and −50 mV in 20-mV increments. In general, we found that the currents relaxed to more negative steady state values with time (Fig. 1, *A* and *B*), implying (*a*) that further channels opened upon hyperpolarization; and (*b*) that the relaxations were progressively larger at more negative test potentials (Fig. 1 *D*). Fig. 1 also illustrates the marked difference in relaxation phenotype for the two receptors, with α3β2 showing relaxations that are briefer in duration (see also Fig. 4) and smaller in amplitude (Fig. 1 *D*) than their α3β4 counterparts at equivalent ACh concentrations.

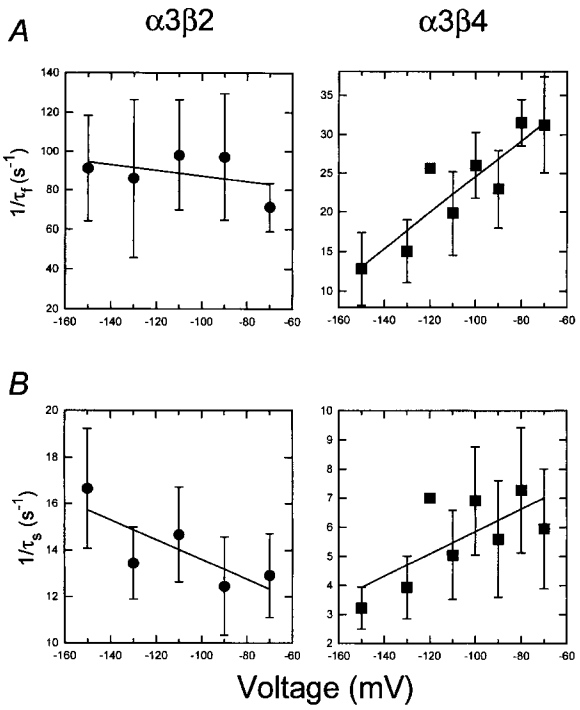

FIGURE 2. Voltage dependence of the relaxation rate constants at [ACh] = 1 μM. Left column, α3β2 receptor; right column, α3β4 receptor. (*A*) Fast rate constants. (*B*) Slow rate constants. Data are mean ± SD, n = 1–10 oocytes. Lines represent linear regression fits through the data points. Slopes are as follows: α3β2 fast component (*A, left*): −0.15 s^{-1}/mV; α3β2 slow component (*B, left*): −0.042 s^{-1}/mV; α3β4 fast component (*A, right*): 0.23 s^{-1}/mV; α3β4 slow component (*B, right*): 0.039 s^{-1}/mV.

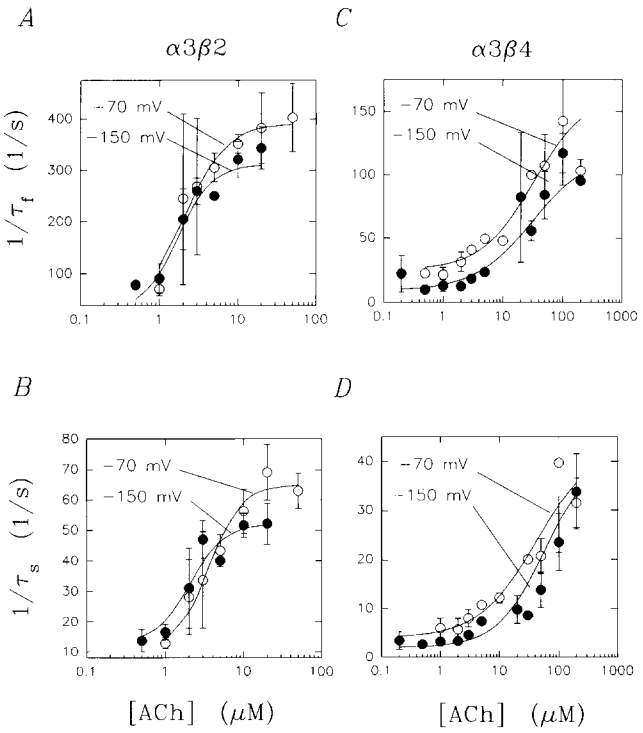

FIGURE 3. The relationships between the relaxation rate constants and [ACh] at membrane potentials of −70 mV (*open circles*) and −150 mV (*filled circles*). (*A*) Fast rate constants for α3β2. (*B*) Slow rate constants for α3β2. (*C*) Fast rate constants for α3β4. (*D*) Slow rate constants for α3β4. Points are mean ± SD (n = 1–10 oocytes). Solid lines are fits to Eq. 1 (see Methods). See Table I for the values of $1/\tau_0$, $1/\tau_{max}$, EC_{50}, and n_{app} for the fitted curves.

These kinetic data can be quantified in several ways. For instance, Fig. 1 *B* shows one- and two-exponential fits to the −150-mV traces in *A*. Whereas the single-exponential fit clearly deviates from the data, the two-exponential curves superimpose on the traces. Two exponentials fit the data, but one did not, at all other voltages and concentrations studied.

The steady state current at the end of the voltage jump (I_{ss}) is the sum of two components: an instantaneous component, I_{inst}, and a relaxation component I_{relax}. I_{inst} is proportional to the number of channels that are available at the prepulse potential (in our case, +50 mV); I_{relax} describes the voltage-dependent opening recruitment of new channels at the test voltage. Steady state current-voltage (*I-V*) relations of neuronal nAChRs typically show steep inward rectification (Ifune and Steinbach, 1990, Ifune and Steinbach, 1992; Sands and Barish, 1992). Our *I-V* data for α3β2 and α3β4 also showed steady state inward rectification. To determine whether I_{inst} or I_{relax} was responsible for the steady state rectification, we plotted the voltage dependence of I_{inst} (Fig. 1 *C*). These relations, obtained by extrapolating the currents to the time of the test jump, showed relatively minor nonlinearities in I_{inst}; the major rectification in the steady state current–voltage relations therefore arises from the kinetically resolvable component I_{relax}.

We investigated the relative sizes of the two relaxation components, I_{inst} and I_{relax}, to compare the relative voltage dependence of the two receptor types. The contribution of the relaxations to the total current can be quantified by plotting the ratio between the instantaneous and steady state values, I_{ss}/I_{inst} (Fig. 1 *D*). In general, α3β4 relaxations are much larger than α3β2 relaxations. Average values for this parameter, from many experiments, are plotted in Fig. 7 below and range from 1.80 at −150 mV to 1.37 at −70 mV for the α3β2 and from 8.61 at −150 mV to 3.08 at −70 mV for the α3β4 receptor.

The different voltage sensitivities of the steady state currents were also reflected by different voltage dependencies of the rate constants (Fig. 2). In general, there were no clear voltage dependencies of the rate constants for the α3β2 receptor, but the α3β4 receptor displayed a roughly twofold change in both the fast and slow rate constants over the range from −70 to −150 mV at 1 μM ACh.

TABLE I

Parameters of the Concentration-Rate Constant Relationship at Different Membrane Potentials

Receptor	Relaxation Component	Potential	$1/\tau_0$	n_{app}	$EC_{50} \pm$ SEE*	$1/\tau_{max} \pm$ SEE*
		mV	s^{-1}		*μM*	s^{-1}
α3β2	Fast	−70	30	1.6	2.1 ± 0.3	362 ± 18
α3β2	Fast	−150	30	1.9	1.7 ± 0.2	288 ± 14
α3β2	Slow	−70	10	2.0	3.5 ± 0.4	55 ± 3
α3β2	Slow	−150	13	2.0	2.1 ± 0.4	39 ± 3
α3β4	Fast	−70	25	1.0	33 ± 14	139 ± 17
α3β4	Fast	−150	9.0	0.9	32 ± 14	109 ± 13
α3β4	Slow	−70	4.0	0.9	42 ± 21	39 ± 7
α3β4	Slow	−150	2.0	1.1	59 ± 20	39 ± 4

We obtained parameters $1/\tau_0$, n_{app}, EC_{50}, and $1/\tau_{max}$ by fitting Eq. 1 to the relaxation data as described in the Methods. The fit provided an error of estimate only for $1/\tau_{max}$ and EC_{50}.
*Standard error of estimate.

Concentration Dependence of Voltage-Jump Kinetics

We measured voltage-jump relaxations over a range of ACh concentrations and membrane potentials for the α3β2 and α3β4 receptors (Fig. 3). There was a clear trend toward more rapid relaxations at higher [ACh], for both exponential components of the relaxations and for both receptors. For the α3β2 receptor, both the fast and slow relaxation rate constants plateaued at an [ACh] > 10 μM (Fig. 3, *A* and *B*). In contrast, the rate constants for the α3β4 receptor did not plateau until the [ACh] approached 1 mM (Fig. 3, *C* and *D*). We fit the data in Fig. 3 to Eq. 1 (see Methods) and obtained the following parameters: the zero-concentration limit $1/\tau_0$, the high-concentration limit $1/\tau_{max}$, the EC_{50}, and the apparent Hill coefficient n_{app}. Membrane potential had little or no effect on these parameters (Table I).

For instance, the EC_{50}'s of the fast α3β2 relaxation were 2.1 ± 0.3 μM (mean ± SEE) at −70 mV and 1.7 ± 0.2 μM at −150 mV; the EC_{50}'s of the slow relaxation were 3.5 ± 0.4 μM at −70 mV and 2.1 ± 0.4 μM at −150 mV. The remaining fit parameters displayed a similar lack of voltage dependence (Table I). The values of $1/\tau_{max}$ for both the fast and slow α3β2 relaxations were ~20–30% less at −150 mV than at −70 mV and the value of $1/\tau_0$ for the fast α3β4 relaxation was ~64% less at −150 than at −70 mV. However, these differences were insignificant compared to the differences between the two subtypes. To simplify comparisons between the wild-type and chimeric receptors and to improve the reliability of the estimated parameters, we pooled the rate constants across voltages (Fig. 4). For the pooled data, the average EC_{50} values for the α3β2 fast and slow phases were 2.3 and 3.1 μM, respectively. For the α3β4 receptor, on the other hand, the average EC_{50} values were 67 and 58 μM. The more rapid kinetics of the α3β2 receptor were reflected in the facts that (*a*) at equal concentrations, α3β2 relaxation profiles were faster than α3β4 relaxations (Fig. 4, *A* and *B*); (*b*) the $1/\tau_0$ values for α3β2 (10 and 50 s^{-1}) were larger than the corresponding values for α3β4 (4 s^{-1} and 15 s^{-1}); and (*c*) the $1/\tau_{max}$ values for α3β2 (50 and 316 s^{-1}) were larger than the corresponding values for α3β4 (36 s^{-1} and 168 s^{-1}).

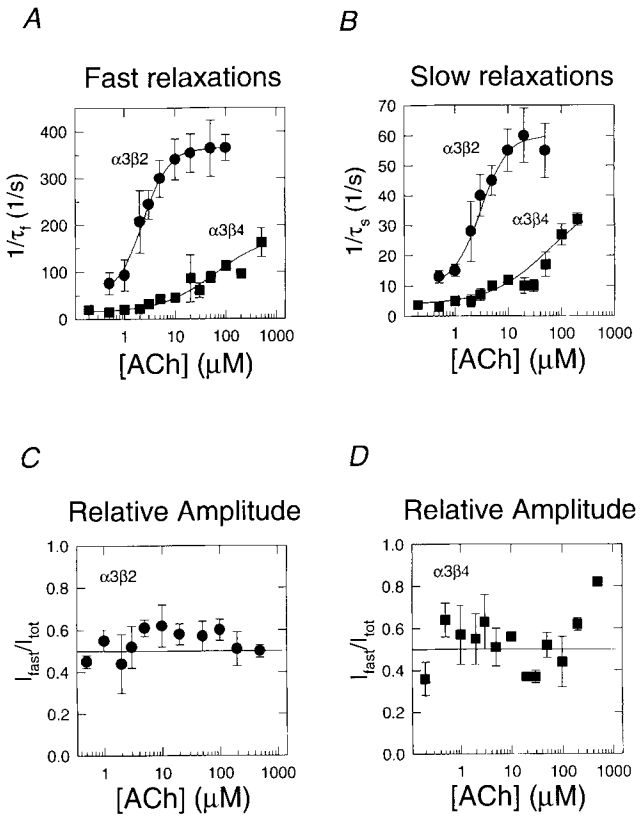

FIGURE 4. Concentration dependence of the voltage-jump kinetics. Data were acquired and analyzed as in Fig. 1 and pooled across all potentials between −50 and −150 mV. The solid lines show EC_{50} values of 2.3 and 3.1 μM for the fast and slow components of the α3β2 receptor; 67 μM and 58 μM for the fast and slow components of the α3β4 receptor; and n_{app} values of 1.7 for both components of the α3β2 relaxations and 0.8 for both components of the α3β4 relaxations. (*A*) Fast phase of the relaxations, $1/\tau_f$. (*B*) Slow phase, $1/\tau_s$. (*C* and *D*) Fractional contribution of the fast phase expressed as I_{fast}/I_{tot}. Points show mean ± SD, n = 2–10 oocytes for each point.

It is thought that the opening rate is relatively independent of voltage; on the other hand, the closing rate is dependent on voltage. Single-channel recordings, however, reveal many types of opening and closing transitions, on times scales ranging from tens of μs to tens of seconds. The observed relaxations, on time scales of milliseconds to hundreds of milliseconds, are generally thought to arise from voltage-dependent

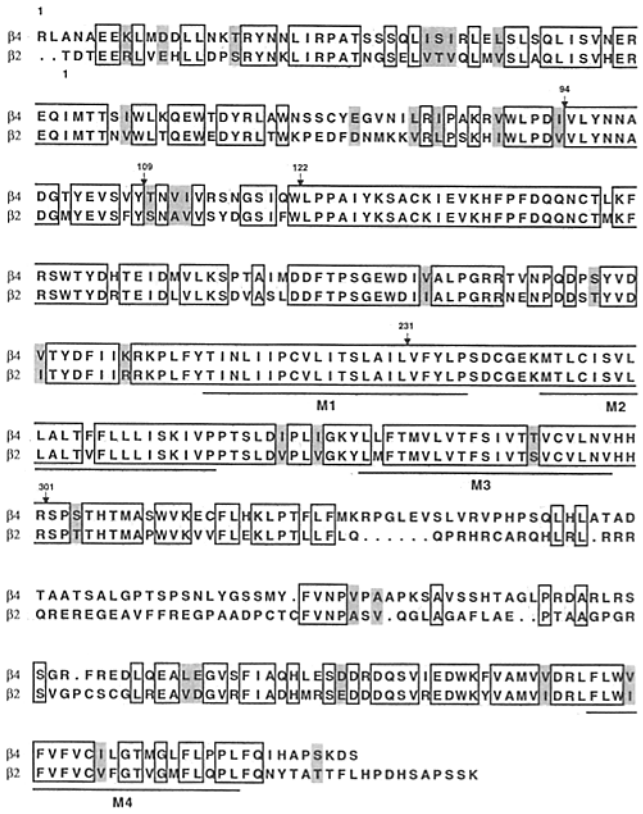

FIGURE 5. Sequence alignment of neuronal nicotinic β2 and β4 subunits. The putative transmembrane regions M1–M4 are underlined. The arrows indicate the transition point of the β4 NH_2-terminal chimeras. The residue preceding the arrow is the last amino acid included from β4. Note the single difference in the M2 transmembrane segments.

burst durations. A burst is thought to arise from binding of a single pair of agonist molecules and to comprise a series of single-channel openings separated by intervals whose time scale is roughly equal to, or shorter than, the duration of the openings. Scheme I predicts a distribution of burst durations that consists of two exponential components (Colquhoun and Hawkes, 1981). We suggest that the low agonist concentration limit of the relaxation rate constants corresponds to the single-channel burst distributions. α3β2 bursts are severalfold briefer than α3β4 bursts, in agreement with this interpretation (Papke et al., 1991). The relaxations are too slow to arise directly from single-channel openings (Charnet et al., 1991; Papke et al., 1991).

The Hill coefficients of the α3β2 receptor were 1.7 for both fast and slow components and 0.8 for both components of the α3β4 receptor. Interestingly, the Hill coefficients for the relaxation dose-response data are roughly the opposite of the values we determined for the steady state dose response relationships (n_H = 1.1 for the α3β2 and n_H = 2.0 for the α3β4 receptors [Cohen et al., 1995]).

Our previous data (Cohen et al., 1995) show that desensitization and channel block cannot account for the differences between the Hill slopes of steady state responses of α3β2 and α3β4. Desensitization and channel block are equally unlikely to account for the differences between the concentration dependence of the relaxation rate constants of α3β2 and α3β4. Desensitization was too slow at [ACh] < 100 μM to cause saturation of the α3β2 relaxation rate constants. Likewise, agonist self-block may have slowed the relaxation rate constants somewhat at [ACh]'s approaching 1 mM (Maconochie and Knight, 1992) but should not cause the relaxation rate constants of α3β2 to approach saturation at ~10 μM.

Each relaxation had two exponential components. Surprisingly, the amplitudes were roughly equal, independent of both (*a*) [ACh] and (*b*) the subunit composition of the receptor (Fig. 4, *C* and *D*). Thus, the global average I_{fast}/I_{tot} was 0.55 ± 0.06 for α3β2 and 0.51 ± 0.10 for α3β4 (mean ± SD, $n > 30$).

Another surprising result of our analysis is that the EC_{50} values for $1/\tau$ do not equal the EC_{50} values for steady state responses reported in a previous study (Cohen et al., 1995). In general, the $1/\tau$ EC_{50} values for both receptors are lower than those for the steady state currents by three- to fourfold. In most straightforward relaxation theories that attempt to obtain equilibrium parameters by kinetics, the EC_{50} for $1/\tau$ equals or exceeds that for equilibrium activation (Adams, 1981). Thus, there remain interesting questions about the molecular and mechanistic details of ACh responses in our experiments. Nonetheless, the concentration dependencies of the kinetic parameters provide a convenient set of metrics for studying the properties of chimeric subunits.

Kinetic Properties of Chimeric β Subunits

We conducted kinetic experiments on a series of β4/β2 subunit chimeras used in a previous study (Cohen et al., 1995). The β4/β2 transition points of these chimeras are presented in Fig. 5. Previous results showed important effects of residues in the region between positions β4 94 and 109 when various β4/β2 subunit chimeras were coexpressed with the α3 subunit. We therefore concentrated our efforts on chimeras in this region.

Fig. 6 presents the concentration dependencies for the relaxation rate constants of three of the chimeras spanning the region that we previously found important in determining the EC_{50} for ACh (Cohen et al., 1995). The rate constants for these chimeras fall within the same general range observed for the wild type receptors: 100 to 350 s^{-1} for the fast rate constants and 20 to 80 s^{-1} for the slow rate constants (data not shown).

We have clarified the data representation by normal-

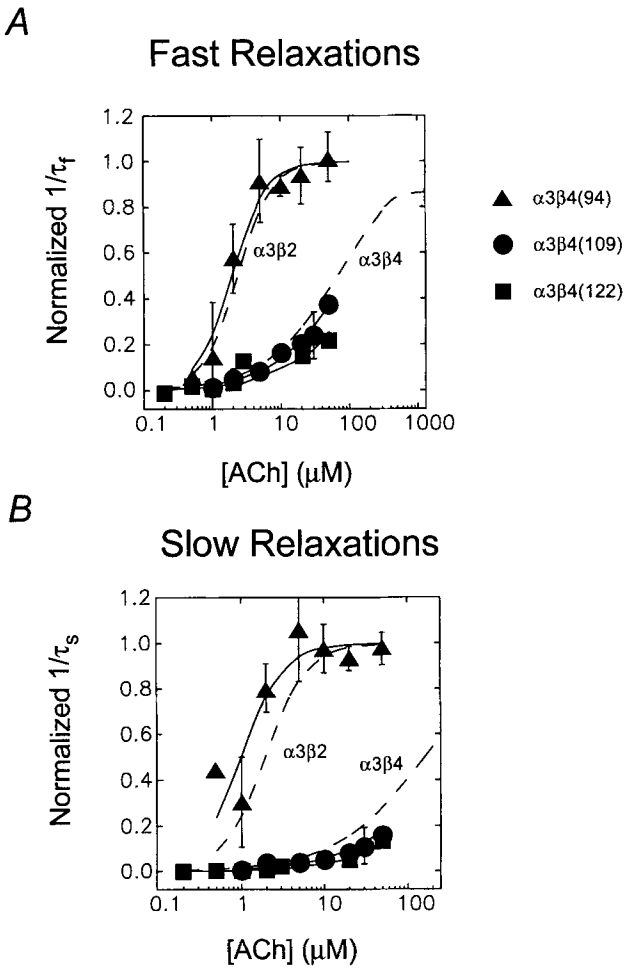

FIGURE 6. Kinetic data for a series of chimeric β subunits. Subtracted and normalized voltage-jump relations, as described in the text. Fast (*A*) and slow (*B*) relaxation components. Solid lines are fitted dose-response relations for the individual receptors; dashed lines are fitted data for α3β2 and α3β4 wild-type receptors. Data for the chimeras are mean ± SD (n = 2–10 oocytes per point). Legend in (*A*) applies to both panels.

izing the concentration dependencies as follows. For each receptor, the dose-response data were fit to the modified Hill equation, Eq. (1) above. The zero-concentration intercepts, $1/\tau_0$, were subtracted, leaving only the concentration-dependent parts of the dose-response relation. Next, the data were normalized by dividing by $1/\tau_{max}$. These subtracted and normalized dose-response relations are plotted in Fig. 6, *A* and *B*, (fast and slow rate constants, respectively). The plots emphasize that the three chimeras segregate into two groups: rate constants for α3β4(94) saturate within the range of concentrations tested, while rate constants for α3β4(109) and for α3β4(122) do not saturate within the range studied and appear shifted toward higher concentrations.

The fitted values for EC_{50} support these impressions: for the fast components, α3β4(94) had an EC_{50} of 1.9 μM, α3β4(109) an EC_{50} of 98 μM and α3β4(122) an EC_{50} of 190 μM. The EC_{50} values for the slow components were 1.0 μM for the α3β4(94), 250 μM for the α3β4(109) and 340 μM for the α3β4(122) receptors. Thus, the EC_{50} values of the relaxation rate constants for α3β4(94) resemble those for α3β2 (2.3 and 3.1 μM for fast and slow relaxations, respectively); whereas the values for α3β4(109) and α3β4(122) chimeras are much greater than those for α3β2. Because the data show little signs of saturation the EC_{50} for the α3β4(109) and α3β4(122) should be considered as roughly comparable to that for the wild type α3β4 receptor.

These results are very similar to our observations with steady state measurements that the dose-response relation shifts rightward by severalfold for the same chimeras within the region 94 to 109 (Cohen et al., 1995). Thus, both our steady state and kinetic data show that a region of β4, spanning residues 94 to 109, is sufficient to shift the EC_{50} of the chimeric receptors from an α3β2 to an α3β4 value. Nonetheless, the absolute values of the kinetic constants themselves do not vary appreciably within this series of chimeras.

Neither Chimeras nor Point Mutations Localize Voltage Dependence or Kinetics

We comment briefly on the extensive kinetic measurements we have made with β4/β2 chimeras in the series of Fig. 5. In all cases, these chimeras displayed (*a*) voltage-dependent steady state responses to ACh, (*b*) voltage-jump relaxations with two exponential components, and (*c*) rate constants for these relaxations in the range of 10 to 400 s^{-1}. Thus, the kinetic phenomenology for the chimeric β subunits falls within the range observed for the two wild-type subunits. However, none of the chimeras we tested approached the unique kinetic and steady state signature of the wild-type α3β4 receptor: slow relaxation rate constants (~3 s^{-1}) leading to severalfold increases in the conductance.

Fig. 7 analyzes steady state voltage dependence by plotting I_{ss}/I_{inst} for several chimeras with progressively longer β4 NH_2 termini. Importantly, there are no major changes in this type of voltage sensitivity within the series that span the range including positions 94 and 109. Therefore, the steady state voltage dependence is not controlled by the same residues that control the EC_{50} for the kinetics. A partial transition to the β4 wild-type phenotype occurs for the α3β4(301) chimera, but its voltage dependence is still much more similar to that of the α3β2 receptor than to that of the α3β4 receptor.

Mutations in the M2 Region

Given the importance of the M2 region for gating of neuronal (Revah et al., 1991) and muscle (Labarca et

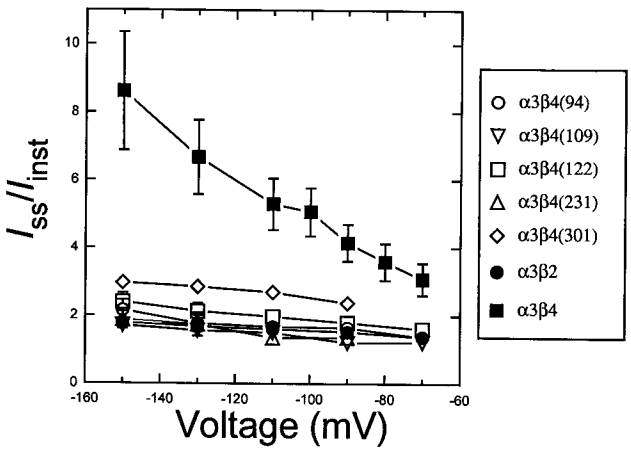

FIGURE 7. Voltage dependence of I_{ss}/I_{inst} for several chimeric β4/β2 receptors, as well as for the wild type β4 and β2 subunits, expressed with the α3 subunit. Analyses as in the experiment of Fig. 1. Data have been pooled from concentrations ranging from 1 to 3 μM ACh. Data are averages of 2–10 cells per point. SEM's are shown where they exceed the size of the symbols.

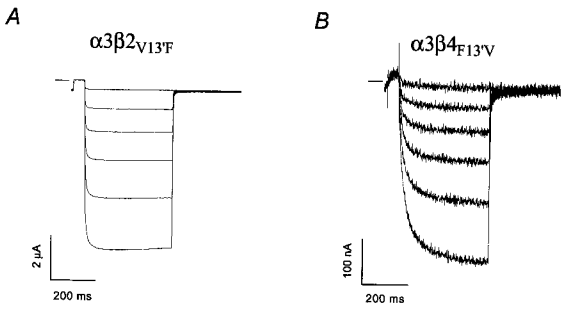

FIGURE 8. Voltage-jump relaxations for (*A*) the $\alpha3\beta2_{V13'F}$ receptor and (*B*) the $\alpha3\beta4_{F13'V}$ receptor. [ACh] = 2 μM. The horizontal bar next to the data denotes zero agonist-induced current. Data were filtered at 500 Hz. The fast relaxation time constants of the $\alpha3\beta2_{V13'F}$ receptor were 4.0, 3.5, 3.1, 2.9, and 2.9 ms at −150, −130, −110, −90, and −70 mV, respectively. The slow relaxation time constants of the $\alpha3\beta2_{V13'F}$ receptor were 21, 20, 18, 18, and 23 ms at −150, −130, −110, −90, and −70 mV, respectively. The fast relaxation time constants of the $\alpha3\beta4_{F13'V}$ receptor were 20, 16, 15, 9.0, and 4.4 ms at −150, −130, −110, −90, and −70 mV, respectively. The slow relaxation time constants of the $\alpha3\beta4_{F13'V}$ receptor are 101, 88, 95, 61, and 71 ms at −150, −130, −110, −90, and −70 mV, respectively.

al., 1995) nAChRs, we were interested in examining the differences between the β2 and β4 subunits within the M2 region. There is only one amino acid substitution in M2 (Fig. 5): β2 has a valine and β4 has a phenylalanine residue at position 13′ (numbering as defined by Charnet et al., 1990). We constructed and tested the appropriate point mutants ($\beta2_{V13'F}$ and $\beta4_{F13'V}$). Fig. 8 shows examples of the $\alpha3\beta2_{V13'F}$ and $\alpha3\beta4_{F13'V}$ relaxation currents in 2 μM ACh. The voltage-jump relaxation phenotypes for these mutants were unchanged from those of the respective wild-type subunits.

DISCUSSION

General Remarks: Role of the β Subunit

The present article describes for the first time a thorough analysis of the voltage-jump relaxation behavior of α3β2 and α3β4 neuronal nAChRs. We describe in detail both the kinetics of voltage-jump relaxations and the concentration dependence of these rate constants. In addition, the study continues our analysis of functional domains of neuronal nAChR β subunits. The present data complement our earlier steady state data (Cohen et al., 1995).

We observe clear differences between the wild type β2 and β4 subunits when coexpressed with the α3 subunit (Fig. 1 and Fig. 4). The α3β2 receptors display less steady state voltage sensitivity relative to the instantaneous current, more rapid kinetics, greater sensitivity to ACh, and a greater Hill coefficient than the α3β4 receptors. The difference in agonist sensitivity was expected from the steady state data; the difference in Hill coefficient is more surprising. Strikingly, the relaxation data complement the steady state data in suggesting that the region between positions 94 and 109 in β4 is crucial in determining agonist binding.

The M2 region of neuronal nicotinic receptors importantly affects gating properties (Revah et al., 1991; Bertrand et al., 1992). The two β subunits we studied differ by only one amino acid in M2 ($\beta2_{13'V}$; $\beta4_{13'F}$), yet this mutation was unable to affect any parameter of the relaxation behavior. We must therefore conclude that the regions that determine subtype differences in the relaxation kinetics are outside M2.

The most straightforward interpretations of the observed relaxation currents are that (*a*) channels open more frequently at more negative potentials, and/or (*b*) the channels remain open for a longer period of time. Although we cannot yet specify the molecular nature of the voltage-dependent rate-limiting gating step that gives rise to the relaxations, it is generally observed that the number of open nAChR channels decreases as the membrane is depolarized (reviewed in Lester, 1992). For muscle receptors, a change in the dipole moment between the open and closed states is thought to give rise to the voltage dependence (Magleby and Stevens, 1972).

Comparisons with Previous Data

Rat neuronal nAChRs in cell lines (Ifune et al., 1992) and in native tissue (Rang, 1981) also display voltage-jump relaxations and neurally evoked postsynaptic currents (PSCs) with two exponential components of approximately equal amplitude. However, the time constants of these components in PC12 cells (4.2 ± 0.8 ms

and 27 ± 5 ms at −100 mV and 20 μM ACh) fall between those for α3β2 and α3β4 under equivalent conditions. The PSC decay time constants in rat submandibular ganglion cells (8 ± 2 ms and 30 ± 5 ms at −70 mV) are somewhat smaller than the τ_o values for α3β2 (20 and 100 ms) and considerably smaller than the α3β4 time constants. The voltage-jump relaxation time constants in rat submandibular ganglion cells at ACh concentrations of 5–15 μM (4–8 ms and 35 ± 2 ms at −70 mV) also lie between our expectations for α3β2 and α3β4 at these ACh concentrations. The differences between the relaxation time constants we measured and those for PC12 and submandibular ganglionic neurons suggest that these cells contain either a receptor subtype that is distinct from the α3β2 and α3β4 receptors or a mixture of the α3β2 and α3β4 receptors.

Previous data suggest that the voltage-jump relaxations for α4β2 expressed in oocytes are monoexponential (Charnet et al., 1991). The voltage-jump relaxation rate constants for α4β2 in 0.2–5 μM ACh (20–40 s^{-1}) are similar to the slow relaxation rate constants we obtained for α3β2 in equivalent ACh concentrations (13–45 s^{-1}). However, recent data show that α4β2 relaxations comprise two exponential components (unpublished data, Cohen, 1995). In 1 μM ACh, the α4β2 relaxation rate constants are similar to those of α3β2. The fast rate constant is 30–50% larger than that of α3β2 and the slow rate constant is about twofold larger than that of α3β2.

In single-channel data (Papke et al., 1991), α3β4 receptors expressed in oocytes have longer burst durations than α3β2 receptors. This observation fits with the longer relaxations for α3β4 in our experiment. However, these burst durations are less than our values for τ_o (Papke et al., 1991). One explanation for this discrepancy is that the α3β2 and α3β4 receptors can rapidly enter a nonconducting state that is outside the direct path of activation during bursts of channel activity. Our maximum rate constant for the fast relaxations for α3β2 is comparable to the rate constant for channel opening for α3β2 estimated by single-channel analysis (Papke et al., 1991).

Single nAChRs in rat neurons display burst distributions that contain two exponential components (Derkach et al., 1987; Mathie et al., 1987; Mathie et al., 1990; Mulle et al., 1992). The fast time constant of the burst distributions is much smaller than the τ_0 values in our experiments. However, the slow time constant for the burst durations are comparable to the fast τ_0 for α3β2 (20 ms): 9 ± 1 ms in superior cervical ganglionic neurons at −110 mV (Derkach et al., 1987), 13 ± 1 ms in sympathetic neurons at −90 to −110 mV (Mathie et al., 1990), and 24 ± 4 ms in neurons in the medial habenular nucleus at −80 mV (Mulle et al., 1992). Nicotinic receptors on bovine chromaffin cells display good agreement between voltage-jump and concentration-jump kinetics (Maconochie et al., 1992). The lower and upper limits of the rate constants in those studies (29 s^{-1} and 460 s^{-1}) agree best with the lower and upper limits of our fast rate constants for α3β2.

Unresolved Issues

What is the physical significance of the two relaxation components? Given our uncertainty about the molecular events that underlie the relaxations, we cannot be certain. Nonetheless, we are struck by the near equality in the amplitudes of the two components over a wide range of [ACh] (Fig. 4, *C* and *D*). We therefore doubt that the two components describe interconvertible states of a single molecule. We suggest instead that the two components reflect distinct, non-interconvertible populations of receptors. The most straightforward, but admittedly daring explanation, is that (*a*) two neuronal nAChR pentamers reside next to each other in the membrane (Zingsheim et al., 1982), (*b*) the two pentamers are slightly asymmetric, and (*c*) the asymmetry reveals itself in our kinetic experiments as a difference in gating behavior. Structural studies are necessary to resolve this issue.

Several aspects of our data are unexpected on the basis of steady state measurements. First, the EC_{50} for the relaxation rate constants are severalfold smaller than the EC_{50} for the steady state currents. Many theories of gating allow for opening rate constants that continue to increase past saturation of the steady state response; but no simple theory predicts that opening rates saturate at concentrations lower than steady state responses. Likewise, we can offer no simple explanation for the fact that the Hill coefficients for the rate constants differ from those for steady state responses: n_{app} is near one for α3β2 steady state currents and for α3β4 rate constants, but near two for α3β4 steady state currents and for α3β2 rate constants.

Acetylcholine receptor gating remains a complex but fascinating problem. For each region identified as important, such as the 94 to 109 region that influences concentration dependence, other phenomena, such as the kinetics and voltage dependence of the process, remain mysterious.

We thank Yinong Zhang, Michael Quick, Mark Nowak, and Craig Doupnik for helpful suggestions, Purnima Deshpande for expert technical help, and Jeremy Gollub, Heather Davis, and Brad Henkle for oocyte preparation and maintenance.

This work was supported by grants from the National Institutes of Health (NS-11756) and from the California Tobacco-Related Disease Research Program (1RT-0365, 1RT-0286).

Original version received 14 August 1995 and accepted version received 13 November 1995.

REFERENCES

Adams, P.R. 1975. Kinetics of agonist conductance changes during hyperpolarization at frog endplates. *Br. J. Pharmacol. Chemo.* 53: 308–310.

Adams, P.R. 1981. Acetylcholine receptor kinetics. *J. Membr. Biol.* 58:161–174.

Bertrand, D., A. Devillers-Thiery, F. Revah, J.-L. Galzi, N. Hussy, C. Mulle, S. Bertrand, M. Ballivet, and J.-P. Changeux. 1992. Unconventional pharmacology of a neuronal nicotinic receptor mutated in the channel domain. *Proc. Natl. Acad. Sci. USA.* 89:1261-1265.

Charnet, P., C. Labarca, R.J. Leonard, N.J. Vogelaar, L. Czyzyk, A. Gouin, N. Davidson, and H.A. Lester. 1990. An open-channel blocker interacts with adjacent turns of α-helices in the nicotinic acetylcholine receptor. *Neuron.* 2:87–95.

Charnet, P., C. Labarca, B.N. Cohen, N. Davidson, H.A. Lester, and G. Pilar. 1991. Pharmacological and kinetic properties of α4β2 neuronal nicotinic acetylcholine receptors expressed in *Xenopus* oocytes. *J. Physiol. (Lond.).* 450:375–394.

Cohen, B.N., A. Figl, M.W. Quick, C. Labarca, N. Davidson, and H.A. Lester. 1995. Regions of β2 and β4 responsible for differences between the equilibrium dose-response relationships of the α3β2 and α3β4 neuronal nicotinic receptors. *J. Gen. Physiol.* 105:745–764.

Colquhoun, D., and A.G. Hawkes. 1981. On the stochastic properties of single ion channels. *Proc. R. Soc. Lond. Biol. Sci.* 211:205–235.

Derkach, V.A., R.A. North, A.A. Selyanko, and V.I. Skok. 1987. Single channels activated by acetylcholine in rat superior cervical ganglion. *J. Physiol. (Lond.).* 388:141–151.

Figl, A., B.N. Cohen, M.W. Quick, N. Davidson, and H.A. Lester. 1992. Regions of β4·β2 subunit chimeras that contribute to the agonist selectivity of neuronal nicotinic receptors. *FEBS Lett.* 308: 245–248.

Figl, A., B.N. Cohen, J. Gollub, N. Davidson, and H.A. Lester. 1993. Novel functional domains of the rat neuronal nicotinic subunit. *Soc. Neurosci. Abstr.* 19:8. (Abstr.)

Guastella, J.G., N. Nelson, H. Nelson, L. Czyzyk, S. Keynan, M.C. Miedel, N. Davidson, H.A. Lester, and B. Kanner. 1990. Cloning and expression of a rat brain GABA transporter. *Science (Wash. DC).* 249:1303–1306.

Higuchi, R. 1990. Recombinant PCR. *In* PCR Protocols, a Guide to Methods and Applications. M.A. Innis, D.H. Gelfand, J.J. Sninsky, and T.J. White, editors. Academic Press, Inc., San Diego, CA. 177–184.

Ifune, C.K., and J.H. Steinbach. 1990. Rectification of acetylcholine-elicited currents in PC12 pheochromocytoma cells. *Proc. Natl. Acad. Sci. USA.* 87:4794–4798.

Ifune, C.K., and J.H. Steinbach. 1992. Inward rectification of acetylcholine-elicited currents in rat phaeochromocytoma cells. *J. Physiol. (Lond.).* 457:143–165.

Labarca, C., M.W. Nowak, H. Zhang, L. Tang, P. Deshpande, and H.A. Lester. 1995. Conserved leucine residues in the M2 domain of nicotinic receptors govern gating independently and symmetrically. *Nature (Lond.).* 376:514–516.

Lester, H.A. 1992. The permeation pathway of neurotransmitter-gated ion channels. *Ann. Rev. Biophys. Biomol. Struct.* 21:267–292.

Luetje, C.W., K. Wada, S. Rogers, S.N. Abramson, K. Tsuji, S. Heinemann, and J. Patrick. 1990. Neurotoxins distinguish between different neuronal nicotinic acetylcholine receptor subunit combinations. *J. Neurochem.* 55:632–640.

Luetje, C.W., and J. Patrick. 1991. Both α- and β-subunits contribute to the agonist sensitivity of neuronal acetylcholine receptors. *J. Neurosci.* 11:837–845.

Maconochie, D.J., and D.E. Knight. 1992. A study of the bovine adrenal chromaffin nicotinic receptor using patch clamp and concentration-jump techniques. *J. Physiol. (Lond.).* 454:129–153.

Magleby, K.L., and C.F. Stevens. 1972. The effect of voltage on the time course of end-plate currents. *J. Physiol. (Lond.).* 223:151–171.

Mathie, A., S.G. Cull-Candy, and D. Colquhoun. 1987. Single-channel and whole-cell currents in dissociated sympathetic neurons in rat. *Proc. R. Soc. Lond. Biol. Sci.* 232:239–248.

Mathie, A., D. Colquhoun, and S.G. Cull-Candy. 1990. Rectification of currents activated by acetylcholine receptors in rat sympathetic ganglion neurons. *J. Physiol. (Lond.).* 427:625–655.

Mulle, C., C. Lena, and J.-P. Changeux. 1992. Potentiation of nicotinic receptor response by external calcium in rat central neurons. *Neuron.* 8:937–945.

Neher, E., and B. Sakmann. 1975. Voltage-dependence of drug-induced conductance in frog neuromuscular junction. *Proc. Natl. Acad. Sci. USA.* 72:2140–2144.

Papke, R.L. 1993. The kinetic properties of neuronal nicotinic receptors: genetic basis of functional diversity. *Progr. Neurobiol.* 41: 509–551.

Papke, R.L., J. Boulter, J. Patrick, and S. Heinemann. 1989. Single-channel currents of rat neuronal nicotinic acetylcholine receptors expressed in *Xenopus* oocytes. *Neuron.* 3:589–596.

Papke, R.L., and S.F. Heinemann. 1991. The role of the β_4 subunit in determining the kinetic properties of rat neuronal nicotinic acetylcholine α_3 receptors. *J. Physiol. (Lond.).* 440:95–112.

Papke, R.L., R.M. Duvoisin, and S.F. Heinemann. 1993. The amino terminal half of the nicotinic-subunit extracellular domain regulates the kinetics of inhibition by neuronal bungarotoxin. *Proc. R. Soc. Lond. Biol. Sci.* 252:141–148.

Quick, M.W., and H.A. Lester. 1994. Methods for expression of excitability proteins in *Xenopus* oocytes. *In* Ion Channels of Excitable Cells. P.M. Conn, editor. Academic Press, San Diego, CA. 261–279.

Rang, H.P. 1981. The characteristics of synaptic currents and responses to acetylcholine of rat submandibular ganglion cells. *J. Physiol. (Lond.).* 311:23–55.

Revah, F., D. Bertrand, J.-L. Galzi, A. Devillers-Thiery, C. Mulle, N. Hussy, S. Bertrand, M. Ballivet, and J.-P. Changeux. 1991. Mutations in the channel domain alter desensitization of a neuronal nicotinic receptor. *Nature (Lond.).* 353:846–849.

Role, L.W. 1992. Diversity in primary structure and function of neuronal nicotinic acetylcholine receptor channels. *Curr. Opin. Neurobiol.* 2:254–262.

Sands, S.B., and M.E. Barish. 1992. Neuronal nicotinic acetylcholine receptor currents in phaeochromocytoma (PC12) cells: dual mechanisms of rectification. *J. Physiol. (Lond.).* 447:467–487.

Sargent, P.B. 1993. The diversity of neuronal nicotinic acetylcholine receptors. *Annu. Rev. Neurosci.* 16:403–443.

Sheridan, R.E., and H.A. Lester. 1975. Relaxation measurements on the acetylcholine receptor. *Proc. Natl. Acad. Sci. USA.* 72:3496–3500.

Vernino, S., M. Amador, C.W. Luetje, J. Patrick, and J.A. Dani. 1992. Calcium modulation and high calcium permeability of neuronal nicotinic acetylcholine receptors. *Neuron.* 8:127–134.

Wong, E.T., S. Mennerick, D.B. Clifford, C.F. Zorumski, and K.E. Isenberg. 1993. Expression of a recombinant neuronal nicotinic acetylcholine receptor in transfected HEK-293 cells. *Soc. Neurosci. Abstr.* 19:291. (Abstr.)

Zingsheim, H.P., D.C. Neugebauer, J. Frank, W. Hanicke, and F.J. Barrantes. 1982. Dimeric arrangement and structure of the membrane-bound acetylcholine receptor studied by electron microscopy. *EMBO J.* 1:541–547.